Citation for final published version:

Garel, F., Goes, S., Davies, R. , Davies, J. H. , Kramer, S. and Wilson, C. 2014. Interaction of subducted slabs with the mantle transition-zone: A regime diagram from 2-D thermo-mechanical models with a mobile trench and an overriding plate. Geochemistry, Geophysics, Geosystems 15 (5) , pp. 1739-1765. 10.1002/2014GC005257

Publishers page: http://dx.doi.org/10.1002/2014GC005257

AUXILIARY MATERIAL for

Interaction of subducted slabs with the mantle transition-zone: a regime diagram from 2-D thermo-mechanical models with a mobile trench and an overriding plate

F. Garel[1,2], S. Goes[1], D. R. Davies[1,3], J. H. Davies[2], S. C. Kramer[1], and C. R. Wilson[4]

[1] *Department of Earth Science and Engineering, Imperial College London, London, UK.*
[2] *School of Earth and Ocean Sciences, Cardiff University, Cardiff, UK.*
[3] *Research School of Earth Sciences, The Australian National University, Canberra, Australia.*
[4] *Lamont-Doherty Earth Observatory, New York, USA.*

Geochemistry, Geophysics and Geosystems

Influence of viscosity jump between upper and lower mantle

Fig. 1 and 2 illustrate the temporal evolution of subducting-plate velocity V_{SP}, trench location and the $V_{\mathrm{OP}}/V_{\mathrm{conv}}$ ratio, for simulations with different viscosity contrasts, $\Delta\mu$, between upper and lower mantle. The range of initial $\mathrm{Age}^0_{\mathrm{SP}}$ and $\mathrm{Age}^0_{\mathrm{OP}}$ summarised in these plots is consistent with the plots shown in Fig. 4 and Fig. 6 of the main text. We clearly observe that trench motion is facilitated by smaller upper-lower-mantle viscosity contrasts. Furthermore, for all but the oldest subducting plate cases, simulations with $\Delta\mu$=100 exhibit a stationary trench later in the model evolution (Fig. 1).

Fig. 2 exhibits oscillations in the $V_{\mathrm{OP}}/V_{\mathrm{conv}}$ ratio during slab-lower-mantle interaction for “ISR” or “BIR” cases. Such oscillations have a larger period and a greater amplitude for $\Delta\mu = 100$ than for $\Delta\mu = 30$, while the oscillations are more subdued for $\Delta\mu = 10$. We interpret this as follows:

1. The more viscous the lower mantle, the more important the slab deformation above it and, thus, the greater the length of slab in the upper mantle. This material sinks at higher velocities than material in the lower mantle, which promotes pulling of the subducting plate and a decrease in the $V_{\mathrm{OP}}/V_{\mathrm{conv}}$ ratio (e.g. between 9 and 20 Myr on Fig. 2 for the case with $\mathrm{Age}^0_{\mathrm{SP}}$=100 Myr, $\mathrm{Age}^0_{\mathrm{OP}}$=20 Myr and $\Delta\mu = 100$).

2. The greater amount of material accumulated in the upper mantle then sinks into the lower mantle (increase of $V_{\mathrm{OP}}/V_{\mathrm{conv}}$ ratio), all the more slowly when $\Delta\mu$ is high, yielding long-period oscillations before a new slab segment in the upper mantle deforms.

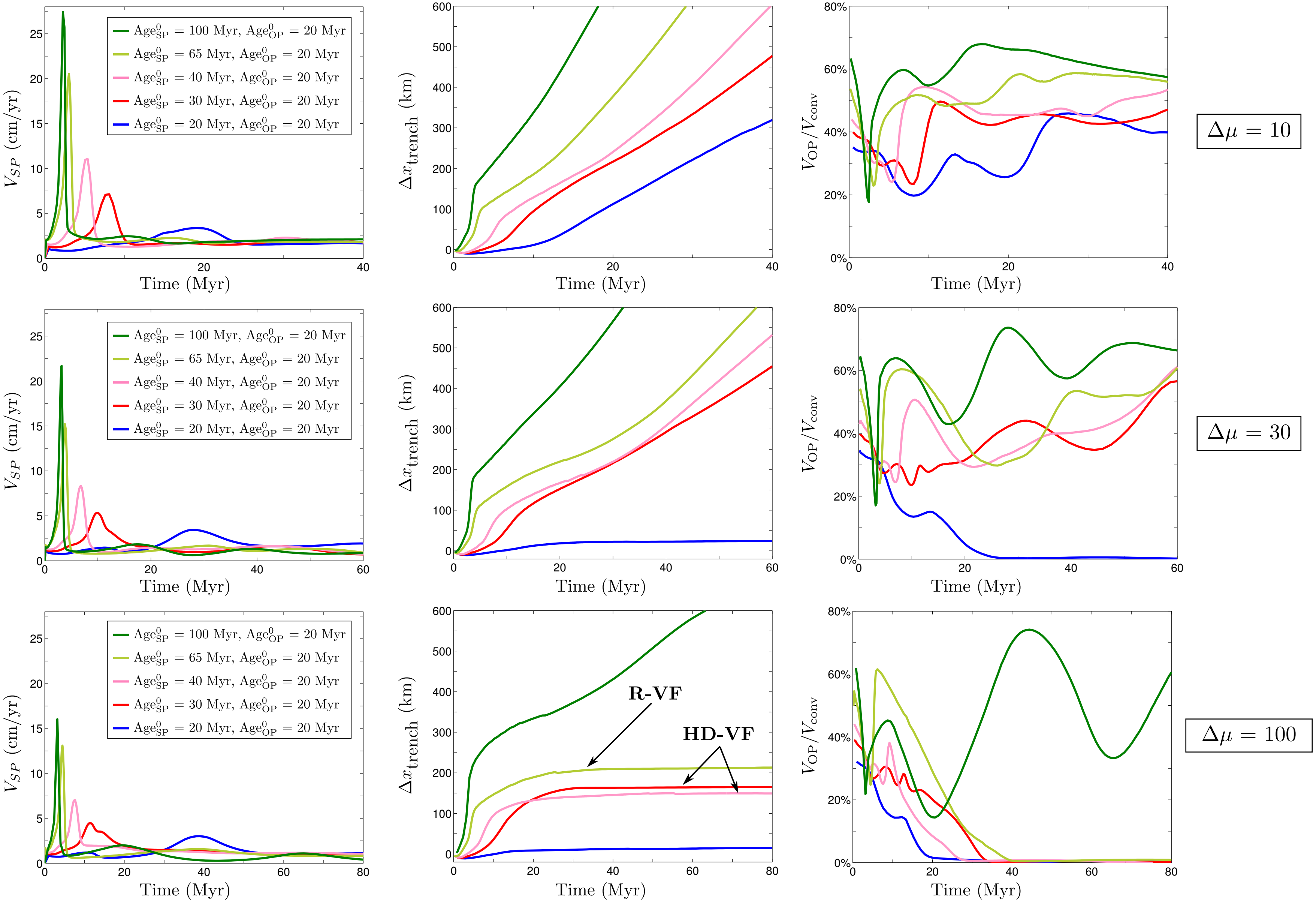

Figure 1: Influence of varying Age$^0_{\mathrm{SP}}$ on the surface dynamics for simulations with a young (20 Myr) overriding plate, for three different viscosity jumps $\Delta\mu$ between upper and lower mantle (10, 30 or 100). Evolution of subducting plate velocities V_{SP} (a), trench retreat $\Delta x_{\mathrm{trench}}$ (b), and $V_{\mathrm{OP}}/V_{\mathrm{conv}}$ (c) as a function of time. Note that the horizontal time scale differs between different $\Delta\mu$ cases. The plots for $\Delta\mu$=30 correspond to Fig. 4 in the main text of the paper.

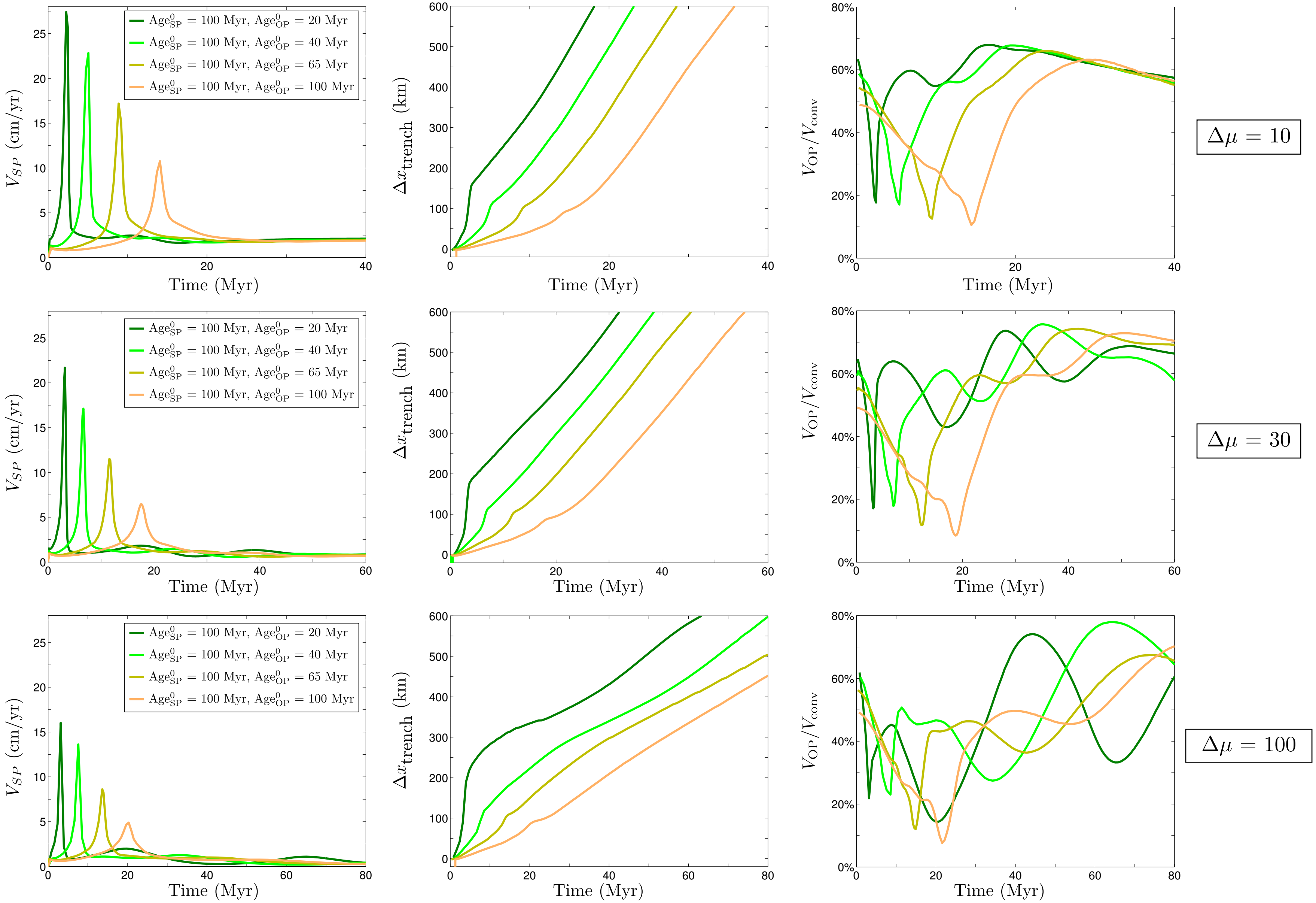

Figure 2: Influence of varying $\mathrm{Age}^0_{\mathrm{OP}}$ on the surface dynamics for simulations with an old (100 Myr) subducting plate, for three different viscosity jumps $\Delta\mu$ between upper and lower mantle (10, 30 or 100). Evolution of subducting plate velocities V_{SP} (a), trench retreat $\Delta x_{\mathrm{trench}}$ (b), and $V_{\mathrm{OP}}/V_{\mathrm{conv}}$ (c) as a function of time. Note that the horizontal time scale differs between different $\Delta\mu$ cases. The plots for $\Delta\mu$=30 correspond to Fig. 6 in the main text of the paper.